Effect of Reinforcement Volume Ratio on Thermal Conductivity of MgO Reinforced Al Matrix Composite Produced by Vacuum Infiltration Method

Ramazan Citak†, Recep Calin* and Zuhtu Pehlivanli‡

Department of Materials and Metallurgy Engineering, Kirikale University, Kirikkale, Turkey
E-mail: recepcalin@hotmail.com

The effect of reinforcement volume ratio on the infiltration behaviour of molten metal, thermal properties and microstructure of Al-MgO composite fabricated by vacuum infiltration method were investigated. Vacuum infiltration is a composite production method in which reinforcement volume ratio is one of important parameters. In this study, MgO powder and Al were used as reinforcement and matrix, respectively. Mixture of MgO and Al powders with 105 mm particle size were filled in quartz tubes freely to form 10, 20 and 30 % reinforcement volume ratio. Liquid Al was vacuum infiltrated into the MgO powder under 550 mmHg vacuum at 730 ± 5 ℃ in normal atmosphere for 3 min. Microstructure of composites were investigated by SEM analysis. From these images, a thermal analysis model has been generated through which the effective thermal conductivity was determined. The effective thermal conductivity of Al-MgO composites increase as the reinforcement volume ratio decreases. The experimental and especially the numerical analysis results in this study gave thermal conductivity values which agree quite well with each other.

Key Words: Composites, Infiltration, MgO, Thermal Conductivity.

INTRODUCTION

Composite materials are developed in the last century and have being used in an increasing ratio. One group of these composite materials is metal matrix composites (MMCs). The demands for high weight materials having high strength and high stiffness have attracted much interest in the development of the fabrication processes for metal matrix composites (MMCs). There are several methods for fabrication of metal matrix composites, such as casting methods, powder metallurgy techniques, *in situ* processes and infiltration methods[1-3]. Infiltration methods have also a few different application techniques[4,5]. These are pressureless (free) infiltration, pressure infiltration and vacuum infiltration techniques. Al_2O_3, TiO_2, SiC and TiC, have been commonly used as reinforcement and many metals and alloys such as

Al, Mg, Ti, Si, Cu, Ni and alloys have been used as matrix. Several process parameters determine whether or not vacuum infiltration occurs and the effect of process parameters such as molten metal temperature, reinforcement powder size, reinforcement volume ratio (RVR), vacuum or pressure value, molten matrix composition, infiltration atmosphere and time are important parameters in infiltration of molten metal into preformed reinforcement. Many studies have been made on these parameters. In infiltration processes reinforcement volume ratio of composites is very important properties. In recent years, metal matrix composites containing high volume fractions of reinforcements have been developed for several applications[6]. Studies on particulate reinforced Al composites produced by infiltration have revealed that the reinforcement volume ratio effects infiltration behaviour and also mechanical and thermal properties in some composites[6-10]. Thermal conductivities of composite materials has recently emerged as an important subject. To measure this, several techniques have been developed recently. The flash technique has been widely used for determining thermal properties over wide ranges of temperatures[11,12]. In this technique, the front surface of a small sample is subjected to a very short burst of high intensity radiant energy. There are other approaches such as numerical techniques in literature[13-16] which calculate these properties, but the main change of principle in the numerical analysis carried out in this study by the use of real SEM images. The microstructure has also significant importance on thermal conductivity behaviour. Several studies were carried out for Si_3N_4 materials[17-21]. The study was also carried out for SiAlON ceramics[22]. Thermal conductivity can be kept under control by means of micro structural modification and the attempt to correlate the microstructures with thermal conductivity behaviour play an important role[23,24]. This can be performed by modeling studies using real microstructure images. However for the application of finite element (FE), the individual intrinsic thermal conductivity values of the consisting phases are required to k_e (effective thermal conductivity) calculated. In this study, the effect of reinforcement volume ratio on thermal conductivity of infiltrated Al-MgO composites has been investigated.

EXPERIMENTAL

Commercially pure magnesia (MgO) and Al with 105 µm particle sizes, have been used as reinforcement and matrix, respectively. The chemical compositions are given in Table-1.

TABLE-1
CHEMICAL COMPOSITION OF MgO AND Al USED IN INFILTRATION TESTS

MgO			
MgO (%)	FeO (%)	SiO_2 (%)	CaO (%)
98	0.6	1.0	0.4

Al								
Si (%)	Fe (%)	Cu (%)	Mn (%)	Ti (%)	Cr (%)	Ni (%)	Pb (%)	Al (%)
0.1	0.4	0.06	0.165	0.022	0.137	0.2	0.062	Balance

Since only pure MgO powder forms 52 % reinforcement volume ratio, MgO and Al powders with 105 μm particulate sizes were mixed and rotate blended for 1 h, to form 10, 20, 30 % reinforcement volume ratio. Infiltration tests have been carried out with quartz tube shown in Fig. 1 with 10 mm outside diameter, 1 mm wall thickness and 300 mm length. Stainless steel filter was placed at the bottom of tube and on the filter Al foil was placed to prevent spillage of powders. Mixture of MgO and Al powders were filled into tube to form 50 mm height freely. To prevent vacuuming of powders, filter, alumina blanket and a weight were placed on the powder. The furnace shown in Fig. 2 was designed and used to melt the matrix metal. Matrix Al has been melted and temperature was kept at 730 ± 5 °C. 550 mmHg vacuum was applied to tube and tube was dipped in liquid metal in normal atmosphere. Vacuum was kept under these conditions for 3 min. After 3 min vacuuming, the tubes were taken out and cooled down in normal atmosphere. Then the tubes were broken and the composites were removed from tubes. Infiltration height were determined. Microstructure of composites were investigated by SEM analysis.
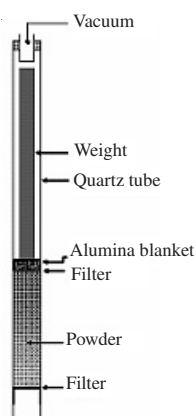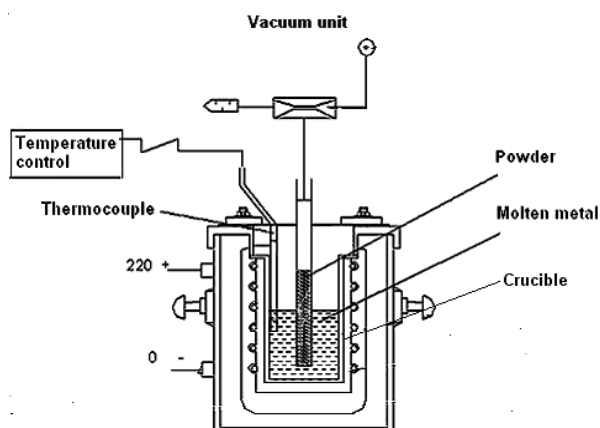

Fig. 1. Infilteration tube   Fig. 2. Vacuum infiltration apparatus

The thermal conductivity values obtained with different analytical models. The used models are known as series (k_s), parallel (k_p), geometric mean (k_g) and Maxwell models. The basic input data in these models are the thermal conductivities and volumetric ratios of the constituent materials. These models are structurally different and depend on the type of material. The numerical model has been set up by transforming the real SEM images of 10, 20 and 30 % reinforcement volume ratio composites. Values of thermal conductivity of composites have been defined by making use of the thermal diffusivity (α) value measured by a marked flashline 2000 laser flash instrument. Schematic illustration of the experimental setup has been given in Fig. 3. The thermal conductivity has been determined using the obtained thermal diffusion coefficient, the density and the specific heat. The numerical model has been set up by transforming the real SEM image.
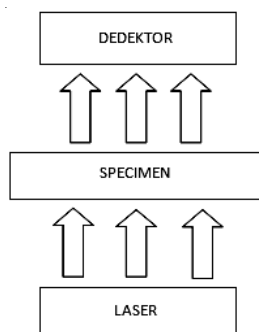
Fig. 3. Schematic illustration measurement of thermal diffusivity by laser flash technique

RESULTS AND DISCUSSION

At 730 ºC, 50 mm infiltration (full infiltration) has been achieved with 10, 20 and 30 % reinforcement volume fractions of 105 μm compact powders. SEM micrograph (Fig. 4) of composites produced with infiltration of different reinforcement ratio. The numerical model has been set up by transforming the real SEM image from Fig. 4.
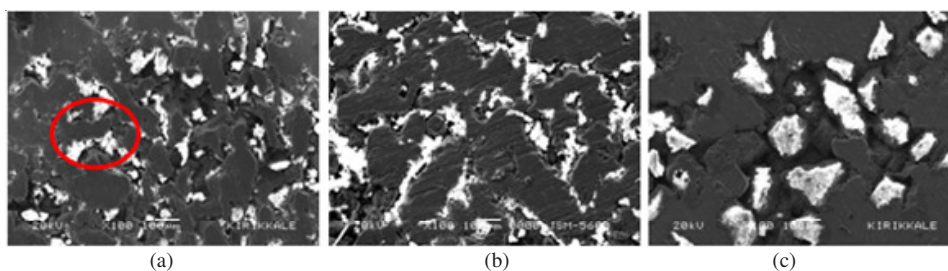

Fig. 4.   SEM micrographs of composite with reinforcement volume ratio
(a) 10 % (b) 20 % (c) 30 %

In this study, all the mentioned models have been employed and the results together with the experimentally measured values are presented in Table-2.

The reinforcement and matrix were drawn with absolute lines by conforming to the original as much as possible. In this way, reinforcement and matrix areas are seen in grey tones in Fig. 5(a) have been clearly formed and the corresponding area ratios have been determined. These determined areas can be thought of as two different materials having separate physical properties. In this way, the problem has been reduced to a stable regime heat transfer of mixed materials having different properties as well as depending on reinforcement volume ratio. The boundary conditions are applied such that there is heat flow only in the horizontal direction and the transverse edges are assumed as adiabatic as shown in Fig. 5(a) and 5(b). Finally, the finite element solution has been obtained using the usual heat transfer procedures.

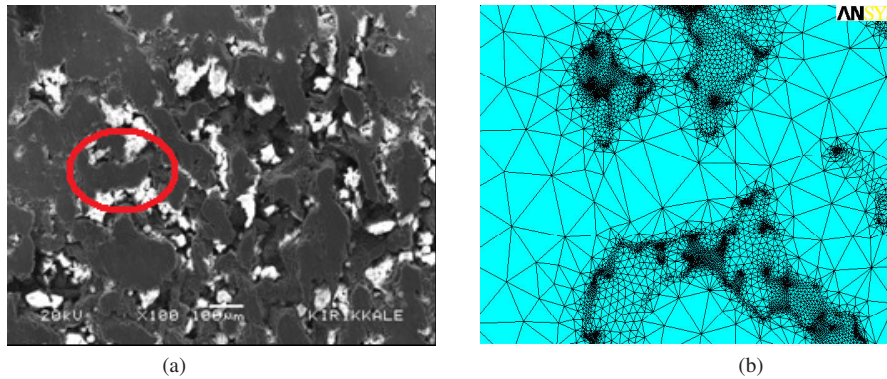(a)   (b)

Fig. 5.   (a) SEM micrographs of composite with reinforcement volume ratio of 10 % and
(b) a piece of the transformed numerical model

Enlarged vector illustration of thermal flux between the phases from the ellipse region is given in Fig. 6. All the results of theoretical models have been employed and the results of experimental measurement are presented in Table-2.
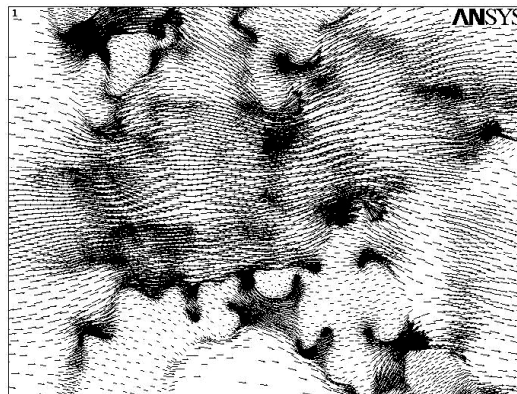

Fig. 6.   Enlarged vectoral illustration of thermal flux between the
phases from the ellipse region

In this study, all the mentioned models have been employed and the results together with the experimentally measured values are presented in Table-2.

TABLE-2
THERMAL CONDUCTIVITY VALUES (W/m K)
OBTAINED WITH DIFFERENT MODELS

RVR	Series (k_s)	Parallel (k_p)	Geometric mean (k_g)	Maxwell (k_x)	Numerical	Experimental
10	131.250	192.00	172.86	185.76	178.64	172.432
20	95.455	174.00	142.29	163.33	138.98	129.589
30	75.000	156.00	117.13	142.50	88.42	87.330

The series and parallel models provide the lower and upper limits of the thermal conductivity, respectively. In Table-3, it can be seen that experimental results that found in this study were between these values. Maxwell which is one of analytical models gave the proximate results to experimental results. Numerical model has given very near results to the experimental results especially for composites with low reinforcement volume ratios. Table-3 also shows that both calculated and experimental thermal conductivities decreased logically with increasing the reinforcement volume ratio because of high thermal resistivity of ceramic particles. Arrows in the Fig. 6 illustrate thermal flux through phases and interphases. The size and density of the arrows represent thermal conductivity and thermal flux, respectively. It can be seen from Fig. 6 that the lowest thermal flux values were provided in the reinforcement. Thermal accumulation and orientation took place in the front of reinforcement colliding with a low conductivity phase from a high conductivity phase. Thermal flux increased in the matrix between two reinforcement phases because of reduction in the matrix section and heat accumulation in this section. The modeling and experimental studies showed that it is possible to set a relationship between the reinforcement volume ratio of composites and the effective thermal conductivity using SEM images of composites with different reinforcement volume ratios.

Conclusion

Effective thermal conductivity has been examined for three different reinforcement volume ratios. The effective thermal conductivity of Al-MgO composites increase towards that of as the reinforcement volume ratio decreases. Experimental results and numerical results are very close to each other and this result is valid for the whole reinforcement volume ratio. The magnitude of the thermal flux is greater in the Al matrix while it is much lower with respect to this value in MgO particles. This situation is directly related to the conductivity coefficients.

Symbols

A_m Al matrix surface area, m^2.

A_f MgO particle surface area, m^2.

c   Specific heat, J/(kg K).

q"   Thermal flux, W/m^2.

k_e Effective thermal conductivity, W/(m K).

k_f Effective thermal conductivity of MgO, W/(m K).

k_s Thermal conductivity of series model $[1/((1-\phi)/k_m + \phi/k_f)]$.

k_g Thermal conductivity of geometric model $[k_m^{(1-\phi)} + k_f^{\phi}]$.

k_m Effective thermal conductivity of Al matrix, W/(m K).

k_x Thermal conductivity of Maxwell and Agari model

$$\left[k_m \cdot \left(\frac{k_f + 2k_m - 2\phi \cdot (k_f - k_m)}{k_f + 2k_m - \phi \cdot (k_f - k_m)} \right) \right].$$

k_p Thermal conductivity of parallel model $[(1-\phi)\cdot k_m + k_f^{\phi})]$.

R   Ratios of Al matrix and MgO thermal conductivities, k_m/k_f.

ϕ Area ratios of Al matrix and MgO A_m/A_f.

α Thermal diffusivity, m^2/s.

ACKNOWLEDGEMENT

REFERENCES

1. D.M. Stefanescu, B.K. Dhindaw and S. Ahuja, *Metallur. Trans.*, **23A**, 2326 (1988).
2. W. Zhou, W. Hu and D. Zhang, *Scripta Mater.*, **39**, 1743 (1998).
3. S.A. Gedeon and I. Tangerini, *Mat. Sci. Eng. A*, **144**, 237, (1991).
4. C.L. Buhrmaster, D.E. Clark and H.O. Smart, *J. Metals*, **40**, 44 (1988).
5. J.A. Martinez, M.I. Pech-Canul, M. Rodríguez-Reyes and J.L. De La Peña, *Mater. Lett.*, **57**, 4332 (2003).
6. J. Wannasin and M.C. Flemings, *J. Mater. Proc. Tech.,* **169**, 143 (2005).
7. M.E.M. Asar, *J. Mater. Proc. Tech.*, **86**, 152 (1998).
8. E. Candan, H.V. Atkinson and H. Jones, *J. Mater. Sci.*, **35**, 4955 (2000).
9. R. Calin and R. Citak, *Mater. Sci. Forum*, **334-356**, 797 (2007).
10. R. Calin and R. Citak, *Mater. Sci. Forum*, **546-549**, 611 (2007).
11. S.L. Casto, E.L. Vqalovo and F. Micari, *J. Mech. Working Tech.*, **20**, 35 (1989).
12. Y.-R. Liu, J.-J. Liu, B.-L. Zhu, Z.-B. Luo and H.-Z. Miao, *Wear*, **210**, 39 (1997).
13. I. Tavman, E. Girgin and R. Klavuz, Proceedings of the 9, Denizli Symposium on Composite Materials (2002).
14. R. Yang and G. Chen, *Phy. Rev. B*, **69**, 195316/1-10 (2004).
15. K. Watari, K. Hirao, M. Toriyama and K. Ishizaki, *J. Am. Ceram. Soc.*, **82**, 777 (1999).
16. K. Hirao, K. Watari, M. E. Brito, M. Toriyama and S. Kanzaki, *J. Am. Ceram. Soc.*, **79**, 2485 (1996).
17. N. Hirosaki, Y. Okamoto, F. Munakata and Y. Akimune, *J. Eur. Ceram. Soc.*, **19**, 2183 (1999).
18. S.W. Lee, H.B. Chae, D.S. Park, Y.H. Choa, K. Niihara and B.J. Hockey, *J. Mater. Sci.*, **35**, 4487 (2000).
19. H. Yokota and M. Ibukiyama, *J. Am. Ceram. Soc.*, **86**, 197 (2003).
20. N. Hirosaki, Y. Okamoto, M. Ando, F. Munakata and Y. Akimune, *J. Am. Ceram. Soc.*, **79**, 2978 (1996).
21. K. Watari, K. Hirao, M. E. Brito, M. Toriyama and K. Ishizaki, *Adv. Tech. Mater. Mater. Proc.*, **7**, 191 (2005).
22. I. Uzun, Z. Pehlivanli and B. Dogan, *Int. J. Eng. Res. Dev.*, **1**, 12 (2009).
23. J.S. Haggerty and A. Lightfoot, *Ceram. Eng. Sci. Proc.*, **16**, 475 (1995).
24. K. Watari, *J. Ceram. Soc. Jpn.*, **109**, 7 (2001).